Spin-blockade effects in spherical quantum dots

R. K. Pandey*
Department of Chemistry, University of California, Irvine, California 92697-2025, USA

Manoj K. Harbola
Physics Department, Indian Institute of Technology Kanpur, Uttar Pradesh 208016, India

Vijay A. Singh
Homi Bhabha Centre for Science Education, Tata Institute of Fundamental Research, V.N. Purav Marg, Mankhurd Mumbai 400088, India

(Received 22 December 2005; revised manuscript received 3 March 2006; published 10 April 2006)

By performing density-functional effective-mass-theory calculations on spherical quantum dots, we show the phenomena of spin blockade effects. It is observed that the spin-blockade depends on the shape of the confinement potential, size of the dot, and depth of the potential.

DOI: 10.1103/PhysRevB.73.165307 PACS number(s): 73.21.La, 73.23.Hk, 73.63.Kv

With novel techniques of fabrication, it is possible to create quantum structures which can confine hundreds of electrons.[1] These systems are known to show some very interesting behavior such as Coulomb-blockade and shell-filling effects.[2–7] In the recent past, a new effect called spin blockade has also been observed in these systems.[8–10] The effect was predicted theoretically for confined two-dimensional (2D) electron gas in a dot[11,12] by Weinmann *et al.* Using a model Hamiltonian approach, they solved the master equation and calculated the dc current using the Landauer formula. As proposed by Weinmann *et al.*[12] there are two kinds of spin-blockade mechanisms. The so-called spin blockade of the first kind, which is related to spin-polarized N-electron states and leads to negative differential conductance. The addition of the electron changes the total spin of the system by 1/2—i.e., $\Delta S=1/2$ in this case. This effect was later described by Franceschetti and Zunger as a violation of the Aufbau principle.[9] They studied the ground-state configuration of an N-electron system in strongly confined InAs, InP, and Si quantum dots (QD's) of diameter $\sim$30 Å. In their study they used pseudopotential single-particle energies and wave functions as input to the many-body expansion of the total energy.

The spin blockade of the second kind is a more general effect and is observed when the total spin of two successive ground states with N and $N+1$ electrons differs by more than 1/2 ($\Delta S>1/2$).[9,12] This leads to a suppression of the conductance in linear and nonlinear transport through a QD. In a recent work, Destefani *et al.*[10] studied spin-blockade effects in a spherical QD. They observed the spin blockade of the first kind in their 3D system and called it an "L blockade" or orbital blockade, which leads to negative differential conductance in linear and nonlinear transport. In addition they also found the spin blockade of the second kind.

Weinmann *et al.* have claimed that both spin effects can be suppressed by a sufficiently high magnetic field. This is supported by experimental work on a single dot[13] and on double dots.[14] On the other hand, Imamura *et al.*[15] in a model calculation based on an exact diagonalization method have predicted that by applying a high magnetic field, the total ground state spin of N and $N+1$ electron QD's can be altered. Thus, the total spin of the two successive ground states is found to alter by more than 1/2 at some specific values of the applied magnetic field. This results in a spin blockade. Also, their results suggest that for magnetic fields higher or lower than these values, a spin blockade is not found. The above predictions are supported by some experimental studies.[16,17] In another work Lee *et al.*[8] studied the effect of hydrogenic impurities on the capacitive energy of a QD. They performed their calculation within the effective mass theory (EMT) and solved the resulting many-electron Schrödinger equation using the local-spin-density approximation (LSDA). By moving the impurity off center they demonstrated the spin-blockade effect for the impurity position intermediate between the center and surface.

In contrast to earlier EMT-LSDA work,[8] we demonstrate spin-blockade effects without an impurity in the QD. In our calculations we take into account the effect of the shape of the confinement potential, which has not been considered in previous calculations, and show that for certain shapes, spin-blockade effects occur. We refer to the spin blockade of the first kind as a strong spin blockade (SSB) and to the spin blockade of the second kind as a weak spin blockade (WSB). We find that spin blockades depend on the shape of the confinement potential, size of the QD, and depth of the potential and that these effects modify the shell structure of the QD.

We choose our model QD to be spherical. The system under consideration has been synthesized by many workers using a colloidal chemistry method.[4] We use the EMT-LSDA methodology in our calculations to solve the Kohn-Sham equation. The Gunnarsson-Lundqvist parametrized form of the exchange correlation potential has been used.[18]

We model the external potential as[6,19]

$$V_{ext}(r)=\begin{cases}(V_0/R^k)r^k-V_0, & r\leqslant R,\\ 0, & r>R,\end{cases} \tag{1}$$

where V_0 is the depth of the potential and can be given by the conduction band offset (valence band offset) between the QD

and the surrounding layer for the electron (hole). R is the radius of the QD. Changing the value of k results in a change of the shape of the potential. In particular $k=2$ is the harmonic confinement case and $k\rightarrow\infty$ is the square well case. We have used effective atomic units, in which $\hbar=m_e=e=1$, and the unit of energy is 27.2 m^*/ϵ^2 eV and that of length (size) is $0.53\epsilon/m^*$ Å, where m^* is the effective mass of the electron inside the QD in units of m_e, the free electron mass, and ϵ is the relative dielectric constant of the material. The calculations were done fully self-consistently using appropriately modified Herman-Skillman code.[20]

There is no general consensus about the shape of the external confinement potential in which N interacting electrons move in a dot. In EMT calculations of the excitonic and optical properties of the QD, the confinement potential is modeled by a square well, in which the barrier posed by the surrounding matrix may be finite or infinite.[21] On the other hand, Coulomb-blockade calculations have been carried out using a harmonic confinement potential.[22,23] There is no rigorous justification for either. Lee *et al.*[24] have reported calculations with anharmonic confinements too. Some studies[25] have indicated that the potential shape is different from these two and plays an important role in determining the abovementioned properties. We note that the electron-hole Coulomb interaction in EMT with a square well has been known to scale as $1/R$. However, an LDA calculation[26] with as many as 800 atoms indicates that the scaling is sublinear $(1/R^{0.7})$. This implies that the many-body physics of the QD would be described better in EMT if the well were neither strictly square nor purely harmonic.

The form of potential we have chosen [Eq. (1)] gives the possibility of tuning the shape of the confinement. For example, if we take the external confinement potential to be parabolic, it means that the N interacting electrons see the background positive charge as uniformly distributed over a sphere of radius R. Similarly, if the background charge density varies linearly from the center of the sphere of radius R towards the surface, then we may assume the confinement shape to be cubic. This is possible by surrounding the QD into a matrix of a material (dielectric or polymer) so that the adhesive force is larger than the cohesive force. Then there may exist a linearly varying background charge density, giving rise to the cubic confinement. If there are excess charges on the surface then the confinement potential may be assumed to be a quasisquare well. Some evidence for a nonuniform background charge density is available from the first-principles calculations of Buda *et al.*[27]

Through our calculations we find spin blockades for $k=3,4,8,10$, etc., but not for $k=1$ and 2. In particular, for $k=3$ (cubic potential), we find that spin-blockade effects are more prominent and are observed over a large variation in the size of the QD and the depth of the confinement potential. However, for $k=4$, 8, and 10 spin blockades occur for large N. This means that spin blockades are observed only when the background charge density is more towards the surface.

The amount of energy needed to add an electron into the dot is known as the capacitive energy or the addition energy, defined as

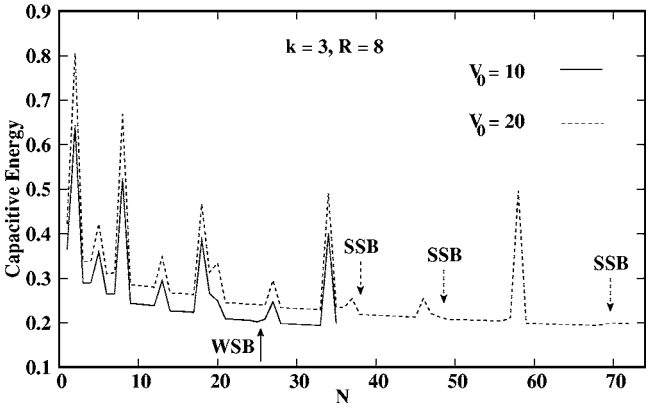

FIG. 1. Capacitive energy $e^2/C(N)$ as a function of the total number of electrons, N, for $k=3$, $R=8$, and $V_0=10$, 20. Electrons are filled according to Hund's rule. The strong- and weak-spin-blockade effects are shown by arrows. Notice that weak spin blockade is suppressed at large V_0.

$$\frac{e^2}{C(N)} = E(N+1) - 2E(N) + E(N-1), \tag{2}$$

where $E(N)$ is the total ground-state energy of an N-electron QD. Note that we are working within EMT and employ constant effective mass of the electron inside the potential well. Nonetheless, employing a constant effective mass is appropriate as long as the wave function tail outside the well is negligibly small. We point out that the depth V_0 employed may take care of both the band offset as well as to some extent the difference in the effective masses inside and outside the well. Reference 21 discusses the complementary role of barrier height and effective masses by introducing a new scale: namely, the mass modified strength of the potential. In Fig. 1, we depict the capacitive energy with the number of electrons, N, added for $k=3$ (cubic potential). Interestingly, both the strong and weak spin blockades are more prominent for the shape index $k=3$. The size R is taken to be 8, and depths of the confinement potential V_0 are 10 and 20. Electrons are filled in the dot according to Hund's rule. Note that for $V_0=10$, the capacitive energy plot exhibits an irregularity at $N=26$. This is the signature of WSB at $N=26$. The electronic structure of the QD with $N=25$ is $1s^2,2p^6,3d^{10},2s^{1\uparrow},2s^{1\downarrow},4f^{5\uparrow}$. The addition of 26th electron changes the electronic structure of the dot as $1s^2,2p^6,3d^{10},2s^{1\uparrow},4f^{7\uparrow}$ $[\Delta S=|S(26)-S(25)|>1/2]$. As V_0 becomes larger, the weak spin blockade disappears and we recover the original shell structure at $N=26$: $1s^2,2p^6,3d^{10},2s^{1\uparrow},2s^{1\downarrow},4f^{6\uparrow}$. In addition to this we also observe SSB. This is found to show up at $N=$ 38, 49, and 70 when V_0 is 20 as indicated in Fig. 1 by arrows.

Figure 2 is also for cubic confinement ($k=3$). We take the size $R=10$ and $V_0=10$, 20. The inset is for $R=12$ and $V_0=10$, 12. We note that both strong and weak spin blockades are observed over a wide range of confinement potential at $R=10$. Notice that the shell structure is destroyed due to spin blockades. It becomes irregular, and the heights of peaks are suppressed. This is due to increase in the exchange-correlation energy. For $R=10$, $V_0=10$, the weak spin block-

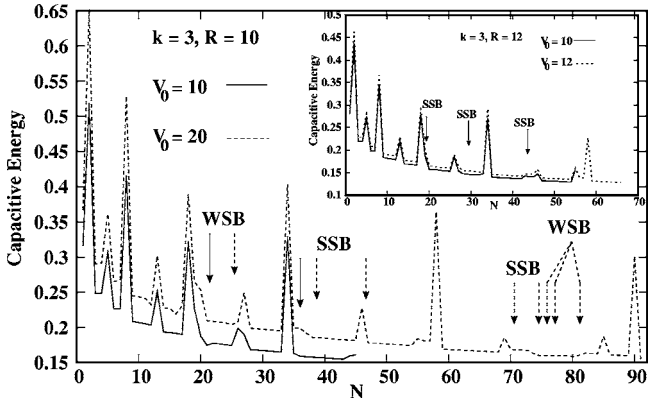

FIG. 2. Capacitive energy $e^2/C(N)$ as a function of the total number of electrons, N, for $k=3$, $R=10$, and $V_0=10,20$. Electrons are filled according to Hund's rule. The inset is for $k=3$, $R=12$, and $V_0=10,12$. Notice that with an increase in the size the weak spin blockade (WSB) is suppressed. However, we still find strong spin blockade (SSB) for this case.

ade occurs at $N=21$. The electronic structure from $N=20$ to $N=21$ changes as $1s^2,2p^6,3d^{10},2s^{1\uparrow},2s^{1\downarrow}$ to $1s^2,2p^6,3d^{10},2s^{1\uparrow},4f^{2\uparrow}$ $[\Delta S=|S(21)-S(20)|>1/2]$. The strong spin blockade occurs at $N=36$. The electronic structure from $N=35$ to $N=36$ changes as $1s^2,2p^6$, $3d^{10},2s^2,4f^{14},3p^{1\uparrow}$ to $1s^2,2p^6,3d^{10},2s^2,4f^{14},3p^{1\uparrow},5g^{1\uparrow}$.

The electronic structure in the case of $R=10$ and $V_0=20$ after the addition of 25th electron is $1s^2,2p^6,3d^{10},2s^{1\uparrow},2s^{1\downarrow},4f^{5\uparrow}$. The addition of a 26th electron causes the $2s^{\downarrow}$ electron to flip its spin and go to the $4f^{\uparrow}$ orbital so that the total ground-state energy is minimized. This happens because the system gains energy in the form of total exchange interaction energy and the corresponding lowering in the electron-electron interaction energy. Consequently the new electronic structure is $1s^2,2p^6,3d^{10},2s^{1\uparrow},4f^{7\uparrow}$, with a total spin change $|S(26)-S(25)|=3/2$ (weak spin blockade). Similarly the electronic structure after the addition of a 37th electron is $1s^2,2p^6,3d^{10},2s^2,4f^{14},3p^{3\uparrow}$. Now the 38th electron does not go to the $3p^{1\downarrow}$ orbital; rather, it goes to the $5g^{1\uparrow}$ orbital. This happens due to the spin blockade of the first kind or strong spin blockade. The new electronic structure is $1s^2,2p^6,3d^{10},2s^2,4f^{14},3p^{3\uparrow},5g^{1\uparrow}$.

The shell-filling sequence for $k=3$, with size $R=10$ and depth of the confinement $V_0=20$, is summarized in Table I. The points where weak spin blockade occurs are marked by a dagger and those points where strong spin blockade occurs are marked by an asterisk. We have observed that the weak spin blockade occurs at $N=26$, when $R=8$ and $V_0=10$ (Fig. 1), but for higher V_0 (=12, 15, and 20) it is not found. Similarly, when $R=10$ and $V_0=10$, the weak spin blockade occurs at $N=21$, but as we increase V_0 it is found to occur at larger and larger N (Fig. 2). For $V_0=12$, 15, and 20 it is observed at $N=22$, 24, and 26, respectively. It is interesting to note that for the case $R=10$, $V_0=20$, the weak spin blockade is found to occur at $N=76$, 78, and 81 also in addition to $N=26$ (Fig. 2 and Table I). As we increase the size further—e.g., at $R=12$—the weak spin blockade disappears (inset of Fig. 2).

When the size is small, $R=8$, the strong spin blockade is found to occur at $N=38$ for $V_0=12$ and at $N=38$, 48 for $V_0=15$. Whereas for $V_0=20$, it is observed at $N=38$, 49, and 70. For intermediate size, $R=10$, the strong spin blockade appears at $N=36$ when $V_0=10$ and at $N=36$, 47 when $V_0=12$, whereas for $V_0=15$ and 20 it is found to be at $N=37$, 47 and $N=38$, 47, 70, 74, respectively (Fig. 2 and Table I). For large size, $R=12$ the strong spin blockade also appears at $N=20$. For $R=12$, $V_0=10$ and 12 it is observed at 20, 30, and 44 (inset of Fig. 2). From these observations we conclude that the spin-blockade effects strongly depend on the size of the dot and the depth of the confinement potential.

TABLE I. The electronic structure of a QD. Cubical confinement potential ($k=3$) is used. We mark with a dagger (†) where weak spin blockade occurs and with an asterisk (*) where strong spin blockade occurs.

$k=3$, $R=10$, $V_0=20$		
N	Electronic structure	ΔS
25	$1s^2,2p^6,3d^{10},2s^{1\uparrow},2s^{1\downarrow},4f^{5\uparrow}$	1/2
26†	$1s^2,2p^6,3d^{10},2s^{1\uparrow},4f^{7\uparrow}$	3/2
37	$1s^2,2p^6,3d^{10},2s^2,4f^{14},3p^{3\uparrow}$	1/2
38*	$1s^2,2p^6,3d^{10},2s^2,4f^{14},3p^{3\uparrow},5g^{1\uparrow}$	1/2
46	$1s^2,2p^6,3d^{10},2s^2,4f^{14},3p^{3\uparrow},5g^{9\uparrow}$	1/2
47*	$1s^2,2p^6,3d^{10},2s^2,4f^{14},3p^{3\uparrow},5g^{9\uparrow},5g^{1\downarrow}$	1/2
58	$1s^2,2p^6,3d^{10},2s^2,4f^{14},3p^{3\uparrow},5g^{9\uparrow},5g^{9\downarrow},3p^{3\downarrow}$	1/2
69	$1s^2,2p^6,3d^{10},2s^2,4f^{14},3p^6,5g^{18},6h^{11\uparrow}$	1/2
70*	$1s^2,2p^6,3d^{10},2s^2,4f^{14},3p^6,5g^{18},6h^{11\uparrow},4d^{1\uparrow}$	1/2
73	$1s^2,2p^6,3d^{10},2s^2,4f^{14},3p^6,5g^{18},6h^{11\uparrow},4d^{4\uparrow}$	1/2
74*	$1s^2,2p^6,3d^{10},2s^2,4f^{14},3p^6,5g^{18},6h^{11\uparrow},4d^{4\uparrow},6h^{1\downarrow}$	1/2
75	$1s^2,2p^6,3d^{10},2s^2,4f^{14},3p^6,5g^{18},6h^{11\uparrow},4d^{4\uparrow},6h^{2\downarrow}$	1/2
76†	$1s^2,2p^6,3d^{10},2s^2,4f^{14},3p^6,5g^{18},6h^{11\uparrow},4d^{3\uparrow},6h^{4\downarrow}$	3/2
77	$1s^2,2p^6,3d^{10},2s^2,4f^{14},3p^6,5g^{18},6h^{11\uparrow},4d^{3\uparrow},6h^{5\downarrow}$	1/2
78†	$1s^2,2p^6,3d^{10},2s^2,4f^{14},3p^6,5g^{18},6h^{11\uparrow},4d^{2\uparrow},6h^{7\downarrow}$	3/2
80	$1s^2,2p^6,3d^{10},2s^2,4f^{14},3p^6,5g^{18},6h^{11\uparrow},4d^{2\uparrow},6h^{9\downarrow}$	1/2
81†	$1s^2,2p^6,3d^{10},2s^2,4f^{14},3p^6,5g^{18},6h^{11\uparrow},4d^{1\uparrow},6h^{11\downarrow}$	3/2
901	$s^2,2p^6,3d^{10},2s^2,4f^{14},3p^6,5g^{18},6h^{11\uparrow},4d^{5\uparrow},6h^{11\downarrow},4d^{5\downarrow}$	1/2
92	$1s^2,2p^6,3d^{10},2s^2,4f^{14},3p^6,5g^{18},6h^{22},4d^{10},7i^{2\uparrow}$	1/2

We find that spin blockade is an exchange-driven phenomenon. However, for large N, the electron correlation may also play an important role. We have verified these by performing our calculations with the exchange-only LSDA, employing the Dirac exchange functional. One such observation is encapsulated in the Table II. Notice from Tables I and II the difference in the electron-filling schemes. We find that only those electronic levels which are nearly degenerate can show weak spin blockade. This should be due to the exchange-driven coupling between the states. Thus an electron with a down spin in one of the states of a system with N electrons flips its spin and goes to the state with the maximum ground state spin of the system with $N+1$ electrons and lowers the energy. However, with the Dirac exchange-only approximation, we observe that the weak spin blockade occurs at different N than when the correlation is included. On the other hand, the number of places where the strong spin blockade takes place remains unchanged. This means that the

TABLE II. The electronic structure of a QD. Cubical confiement potential ($k=3$) is used. We mark with a dagger (†) where weak spin blockade occurs and with an asterisk (*) where strong spin blockade occurs. Calculations are performed using Dirac exchange only the LSDA.

$k=3$, $R=10$, $V_0=20$		
N	Electronic structure	ΔS
23	$1s^2,2p^6,3d^{10},2s^{1\uparrow},2s^{1\downarrow},4f^{3\uparrow}$	1/2
24†	$1s^2,2p^6,3d^{10},2s^{1\uparrow},4f^{5\uparrow}$	3/2
37	$1s^2,2p^6,3d^{10},2s^2,4f^{14},3p^{3\uparrow}$	1/2
38*	$1s^2,2p^6,3d^{10},2s^2,4f^{14},3p^{3\uparrow},5g^{1\uparrow}$	1/2
46	$1s^2,2p^6,3d^{10},2s^2,4f^{14},3p^{3\uparrow},5g^{9\uparrow}$	1/2
47*	$1s^2,2p^6,3d^{10},2s^2,4f^{14},3p^{3\uparrow},5g^{9\uparrow},5g^{1\downarrow}$	1/2
58	$1s^2,2p^6,3d^{10},2s^2,4f^{14},3p^{3\uparrow},5g^{9\uparrow},5g^{9\downarrow},3p^{3\downarrow}$	1/2
69	$1s^2,2p^6,3d^{10},2s^2,4f^{14},3p^6,5g^{18},6h^{11\uparrow}$	1/2
70*	$1s^2,2p^6,3d^{10},2s^2,4f^{14},3p^6,5g^{18},6h^{11\uparrow},4d^{1\uparrow}$	1/2
74	$1s^2,2p^6,3d^{10},2s^2,4f^{14},3p^6,5g^{18},6h^{11\uparrow},4d^{5\uparrow}$	1/2
75	$1s^2,2p^6,3d^{10},2s^2,4f^{14},3p^6,5g^{18},6h^{11\uparrow},4d^{5\uparrow},6h^{1\downarrow}$	1/2
80	$1s^2,2p^6,3d^{10},2s^2,4f^{14},3p^6,5g^{18},6h^{11\uparrow},4d^{5\uparrow},6h^{6\downarrow}$	1/2
81†	$1s^2,2p^6,3d^{10},2s^2,4f^{14},3p^6,5g^{18},6h^{11\uparrow},4d^{4\uparrow},6h^{8\downarrow}$	3/2
82†	$1s^2,2p^6,3d^{10},2s^2,4f^{14},3p^6,5g^{18},6h^{11\uparrow},4d^{3\uparrow},6h^{10\downarrow}$	3/2
83	$1s^2,2p^6,3d^{10},2s^2,4f^{14},3p^6,5g^{18},6h^{11\uparrow},4d^{3\uparrow},6h^{11\downarrow}$	1/2
91	$1s^2,2p^6,3d^{10},2s^2,4f^{14},3p^6,5g^{18},6h^{22},4d^{10},7i^{1\uparrow}$	1/2

inclusion of correlation (in our case we have used the Gunnarsson-Lundqvist parametrized form) affects the electron-filling scheme in that it shifts the weak spin blockade. It also induces the additional strong (at $N=74$) and weak (at $N=76$) spin blockades (see Tables I and II for a comparison of the electronic structure within the correlation-included LSDA and the exchange-only LSDA). As stated earlier, for large N, the electron correlation may also play an important role in spin-blockade effects. In this connection we point out that within the correlation-included LSDA, the strong spin blockade occurs at $N=74$ (see Table I), where the 74th electron does not occupy the $4d^{\uparrow}$ orbital but rather it occupies the $6h^{\downarrow}$ orbital. This is against Hund's rule. On the other hand, within the Dirac exchange-only LSDA, the 74th electron occupies the $4d^{\uparrow}$ orbital (see Table II). In a recent work[28] the violation of Hund's rule in spherical QD's, under applied magnetic field, has been discussed. We note that the higher levels in the dot are very close in energy and therefore they strongly mix together. This may lead to a reordering of levels.

Both strong and weak spin blockades are observed for intermediate size (e.g., $R=10$) and larger depths of confinement so that more electrons can be accommodated into the dot. Spin-blockade effects depend on the shape of the confinement (that is, the way the background positive charge is distributed in a dot), size of the dot, and depth of the confinement (that is, the gate voltage applied to a single-electron transistor). The weak spin blockade can be suppressed when the size of the QD is small and the depth of the confinement is large (since the levels are no longer nearly degenerate) as shown in Fig. 1. For small sizes the degeneracy between the

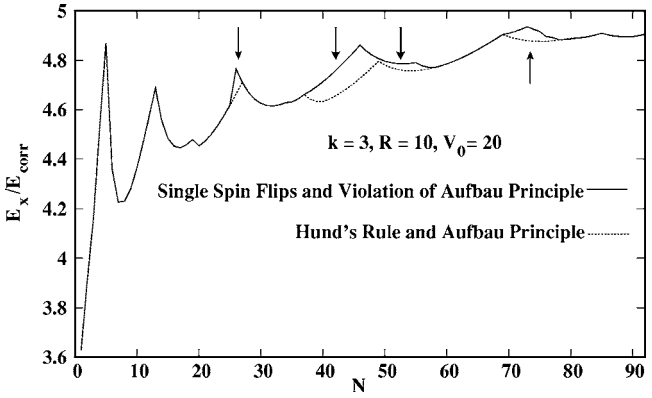

FIG. 3. The ratio of total exchange energy to total correlation energy (E_x/E_{corr}) is depicted as a function of total number of electrons (N) for the case $k=3$, $R=10$, and $V_0=20$. The dashed line shows the case when electrons are filled according to Hund's rule and the Aufbau principle, whereas the solid line shows the case in which a single spin flip gives rise to weak spin blockade and violation of the Aufbau principle gives rise to strong spin blockade. The weak-spin-blockade regions are shown by thin arrows whereas the strong-spin-blockade regions are shown by thick arrows.

$4f$ and $2s$ states is lifted, because the $4f$ wave function is more spread out. At very large sizes also, the weak spin blockade is suppressed no matter how small or large depth of the confinement we chose, as shown in the inset of Fig. 2.

To get a better understanding of our observation of spin blockade effects, we plot in Fig. 3 the ratio of the total exchange energy to the correlation energy of the electrons in a QD as a function of the number of electrons in it. The parameters chosen are $k=3$, $R=10$, and $V_0=20$. The dashed line shows the case when electrons are filled according to Hund's rule and the Aufbau principle, whereas the solid line shows the case in which a single spin flip[9] (for the minimum-energy configuration; the two energies are different when spin blockade occurs) and violation of the Aufbau principle give rise to weak and strong spin blockades, respectively. As is clearly seen, the magnitude of exchange energy is maximum when the shell is half filled in both cases. However, notice the dramatic increase in the exchange energy where the spin blockades occur. The exchange-driven coupling between the two electronic levels which are fraction of a meV apart may lead to spin blockades. The difference in the total ground-state energy between the two schemes of Fig. 3 is equal to the spin-blockade energy. However, the strength of strong-spin-blockade energy is larger than the weak-spin-blockade energy by roughly an order of magnitude and varies from material to material. The magnitude of weak-spin-blockade energy varies from 0.01 meV to 1 meV, whereas the magnitude of strong-spin-blockade energy varies from 0.1 meV to 10 meV. Table III lists typical weak- and strong-spin-blockade energies for different materials.

In conclusion we have demonstrated that spin blockade may be observed depending on the system, its size, and the environment chosen. Imamura *et al.*[15] found the spin-blockade effect by varying the magnetic field. Lee *et al.*[8] have shown that moving a hydrogenic impurity off center

TABLE III. Typical weak-spin-blockade energy at $N=26$ for different materials and for $k=3$, $R=8$, and $V_0=10$. The strong-spin-blockade energy at $N=38$ is listed for different materials and for $k=3$, $R=8$, and $V_0=12$.

Material	R (nm)	V_0 (eV)	WSB energy (meV)	V_0 (eV)	SSB energy (meV)
GaAs	79.6	0.115	0.035	0.138	0.384
InP	71.8	0.130	0.039	0.156	0.434
CdSe	30.0	0.418	0.125	0.501	1.395
Si	24.8	0.397	0.119	0.476	1.333
CdS	11.7	1.80	0.539	2.16	6.005
ZnS	5.8	2.23	0.669	2.68	7.455

results in spin blockade. In our case we have varied the shape of the confinement corresponding to the shape index k [Eq. (1)], size, and depth of the potential and shown that spin blockade may occur for $k \geqslant 3$. In particular spin blockade is more prominent for the case when $k=3$ and is observed over a wide range of size and depth of the confinement. We have found that spin blockades (both strong and weak) are exchange-driven phenomena and that both depend on the shape of the potential, size of the dot, and depth of the confinement. Weinmann *et al.*[12] have suggested that the spin-blockade effect can be suppressed by applying a sufficiently high magnetic field. We have shown that the weak spin blockade can be suppressed if the size of the dot is small and depth of the potential is large. On the other hand, if the size is very large, then independent of the depth of the confinement potential, the weak spin blockade can be suppressed.

*Electronic address: pandeyr@uci.edu

[1] R. C. Ashoori, Nature (London) **379**, 413 (1996).
[2] G. J. Iafrate, K. Hess, J. B. Krieger, and M. Macucci, Phys. Rev. B **52**, 10737 (1995).
[3] S. Tarucha, D. G. Austing, T. Honda, R. J. van der Hage, and L. P. Kouwenhoven, Phys. Rev. Lett. **77**, 3613 (1996).
[4] D. L. Klein, R. Roth, A. Lim, A. P. Alivisatos, and P. L. McEuen, Nature (London) **389**, 699 (1997).
[5] M. Macucci, K. Hess, and G. J. Iafrate, Phys. Rev. B **55**, R4879 (1997).
[6] V. Ranjan, R. K. Pandey, M. K. Harbola, and V. A. Singh, Phys. Rev. B **65**, 045311 (2002).
[7] S. M. Riemann and M. Manninen, Rev. Mod. Phys. **74**, 1283 (2002).
[8] I.-H. Lee, K.-H. Ahn, Y.-H. Kim, R. M. Martin, and J. P. Leburton, Phys. Rev. B **60**, 13720 (1999).
[9] A. Franceschetti and A. Zunger, Europhys. Lett. **50**, 243 (2000).
[10] C. F. Destefani, G. E. Marques, and C. Trallero-Giner, Phys. Rev. B **65**, 235314 (2002).
[11] D. Weinmann, W. Hausler, W. Pfaff, B. Kramer, and U. Weiss, Europhys. Lett. **26**, 467 (1994).
[12] D. Weinmann, W. Hausler, and B. Kramer, Phys. Rev. Lett. **74**, 984 (1995).
[13] A. K. Huttel, H. Qin, A. W. Holleitner, R. H. Blick, K. Neumaier, D. Weinmann, K. Eberl, and J. P. Kotthaus, Europhys. Lett. **62**, 712 (2003).
[14] K. Ono, D. Austing, Y. Tokura, and S. Tarucha, Science **297**, 1313 (2002).
[15] H. Imamura, H. Aoki, and P. A. Maksym, Phys. Rev. B **57**, R4257 (1998).
[16] M. Ciorga, A. S. Sachrajda, P. Hawrylak, C. Gould, P. Zawadzki, S. Jullian, Y. Feng, and Z. Wasilewski, Phys. Rev. B **61**, R16315 (2000).
[17] L. P. Rokhinson, L. J. Guo, S. Y. Chou, and D. C. Tsui, Phys. Rev. B **63**, 035321 (2001).
[18] O. Gunnarsson and B. I. Lundqvist, Phys. Rev. B **13**, 4274 (1976).
[19] R. K. Pandey, M. K. Harbola, and V. A. Singh, Phys. Rev. B **67**, 075315 (2003).
[20] F. Herman and S. Skillman, *Atomic Structure Calculation* (Prentice-Hall, Englewood Cliffs, NJ, 1963).
[21] M. Singh, V. Ranjan, and V. A. Singh, Int. J. Mod. Phys. B **14**, 1753 (2000).
[22] M. Macucci, K. Hess, and G. J. Iafrate, J. Appl. Phys. **77**, 3267 (1995).
[23] L. R. C. Fonseca, J. L. Jimenez, J. P. Leburton, and R. M. Martin, Phys. Rev. B **57**, 4017 (1998).
[24] I.-H. Lee, V. Rao, R. M. Martin, and J. P. Leburton, Phys. Rev. B **57**, 9035 (1998).
[25] J. Adamowski, M. Sobkowicz, B. Szafran, and S. Bednarek, Phys. Rev. B **62**, 4234 (2000).
[26] S. Ogut, J. R. Chelikowski, and S. G. Louie, Phys. Rev. Lett. **79**, 1770 (1997).
[27] F. Buda, J. Kohanoff, and M. Parrinello, Phys. Rev. Lett. **69**, 1272 (1992).
[28] C. F. Destefani, J. D. M. Vianna, and G. E. Marques, Semicond. Sci. Technol. **19**, L90 (2004).